



**HAL**  
open science

## Water balance modelling in a tropical watershed under deciduous forest (Mule Hole, India): Regolith matrix storage buffers the groundwater recharge process

Laurent Ruiz, M.R.R. Varma, M.S. Mohan Kumar, Muddu Sekhar, Jean-Christophe Maréchal, Marc Descloitres, Jean Riotte, Sat Kumar, C. Kumar, Jean-Jacques Braun

### ► To cite this version:

Laurent Ruiz, M.R.R. Varma, M.S. Mohan Kumar, Muddu Sekhar, Jean-Christophe Maréchal, et al.. Water balance modelling in a tropical watershed under deciduous forest (Mule Hole, India): Regolith matrix storage buffers the groundwater recharge process. *Journal of Hydrology*, 2010, 380 (3-4), pp.460-472. 10.1016/j.jhydrol.2009.11.020 . hal-00462049

**HAL Id: hal-00462049**

**<https://hal.science/hal-00462049>**

Submitted on 8 Mar 2010

**HAL** is a multi-disciplinary open access archive for the deposit and dissemination of scientific research documents, whether they are published or not. The documents may come from teaching and research institutions in France or abroad, or from public or private research centers.

L'archive ouverte pluridisciplinaire **HAL**, est destinée au dépôt et à la diffusion de documents scientifiques de niveau recherche, publiés ou non, émanant des établissements d'enseignement et de recherche français ou étrangers, des laboratoires publics ou privés.

1 **Water balance modelling in a tropical watershed under deciduous forest**  
2 **(Mule Hole, India) : regolith matrix storage buffers the groundwater**  
3 **recharge process**

4

5 Laurent Ruiz<sup>a,b,\*</sup>, Murari R. R. Varma<sup>c,d</sup>, M. S. Mohan Kumar<sup>c,d</sup>, M. Sekhar<sup>c,d</sup>, Jean-  
6 Christophe Maréchal<sup>c,e,f,g</sup>, Marc Descloitres<sup>c,h</sup> Jean Riotte<sup>c,e,f,g</sup> and Jean-Jacques Braun<sup>c,e,f,g</sup>

7

8 <sup>a</sup> INRA, UMR1069, Sol Agro et hydrosystème Spatialisation, 35000 Rennes, France

9 <sup>b</sup> Agrocampus Ouest, UMR1069, Sol Agro et hydrosystème Spatialisation, 35000 Rennes,  
10 France

11 <sup>c</sup> Indo-French Cell for Water Sciences, IISc-IRD Joint laboratory, Indian Institute of Science,  
12 560012 Bangalore, India

13 <sup>d</sup> Indian Institute of Science, Department of Civil Engineering, , Bangalore 560 012, INDIA

14 <sup>e</sup> Université de Toulouse ; UPS (OMP) ; LMTG; 14 Av Edouard Belin, F-31400 Toulouse,  
15 France

16 <sup>f</sup> CNRS ; LMTG ; F-31400 Toulouse, France

17 <sup>g</sup> IRD ; LMTG ; F-31400 Toulouse, France

18 <sup>h</sup> IRD ; Université de Grenoble ; CNRS ; LTHE , BP53, 38041 Grenoble, Cedex 9, France

19

20

21 \* corresponding author:

22 Laurent RUIZ, INRA, Sol Agro and hydroSystemes, 4 rue Stang Vihan, F-29000 Quimper,  
23 France

24 E-mail : [ruiz@rennes.inra.fr](mailto:ruiz@rennes.inra.fr)

25 Tél : +33 (0) 2 98 95 99 64

26 **Abstract**

27

28 Accurate estimations of water balance are needed in semi-arid and sub-humid tropical  
29 regions, where water resources are scarce compared to water demand. Evapotranspiration  
30 plays a major role in this context, and the difficulty to quantify it precisely leads to major  
31 uncertainties in the groundwater recharge assessment, especially in forested catchments. In  
32 this paper, we propose a lumped conceptual model (COMFORT), which accounts for the  
33 water uptake by deep roots in the unsaturated regolith zone. The model is calibrated using a  
34 five year hydrological monitoring of an experimental watershed under dry deciduous forest in  
35 South India (Mule Hole watershed).

36

37 The model was able to simulate the stream discharge as well as the contrasted behaviour of  
38 groundwater table along the hillslope. Water balance simulated for a 32 year climatic time  
39 series displayed a large year-to-year variability, with alternance of dry and wet phases with a  
40 time period of approximately 14 years. On an average, input by the rainfall was 1090  
41  $\text{mm}\cdot\text{year}^{-1}$  and the evapotranspiration was about 900  $\text{mm}\cdot\text{year}^{-1}$  out of which 100  $\text{mm}\cdot\text{year}^{-1}$   
42 was uptake from the deep saprolite horizons. The stream flow was 100  $\text{mm}\cdot\text{year}^{-1}$  while the  
43 groundwater underflow was 80  $\text{mm}\cdot\text{year}^{-1}$ .

44

45 The simulation results suggest that i) deciduous trees can uptake a significant amount of water  
46 from the deep regolith, ii) this uptake, combined with the spatial variability of regolith depth,  
47 can account for the variable lag time between drainage events and groundwater rise observed  
48 for the different piezometers, iii) water table response to recharge is buffered due to the long  
49 vertical travel time through the deep vadose zone, which constitutes a major water reservoir.

50 This study stresses the importance of long term observatories for the understanding of  
51 hydrological processes in tropical forested ecosystems.

52

53 **Key Words:** matric porosity, groundwater recharge, lumped model, semi-arid tropics,  
54 evapotranspiration, vadose zone, forested watershed hydrology.

55

## 56 **Introduction**

57

58 Accurate assessment of water balance at the watershed scale is of major importance in a  
59 context of a global dramatic increase of human demand for water, either for urban or  
60 agricultural requirements. This assessment is complex, since water balance results from the  
61 interaction of climate, geology, morphology, soil and vegetation (De Vries and Simmers,  
62 2002).

63 A large suit of rainfall-runoff models are available that are either fully empirical or  
64 mechanistic, which make it possible to predict with reasonable accuracy water balance from  
65 watersheds in temperate climates (Beven, 2001 ; Wagener et al., 2004). These models are  
66 usually evaluated according to their ability to simulate stream discharge. In semi-arid or arid  
67 climates, calibration of watershed models is difficult because streams are often ephemeral.  
68 Moreover, as potential evapotranspiration equals or surpasses average precipitation, a correct  
69 evaluation of actual evapotranspiration becomes crucial (Scanlon et al., 2002, 2006 ; Sekhar  
70 et al., 2004 ; Anuraga et al., 2006). Despite the large amount of work dedicated to assess  
71 evapotranspiration at the watershed scale, this flux remains the largest source of uncertainty  
72 in water budgeting, especially in the case of forested watersheds (Zhang et al., 2001; 2004).

73

74 The objective of this paper is to propose a methodology for water balance estimation in a  
75 tropical forested watershed, based on the calibration of a conceptual model against stream  
76 discharge and groundwater level data. The experimental watershed used in this study was  
77 developed as part of the project “Observatoire de Recherche en Environnement – Bassin  
78 Versant Expérimentaux Tropicaux” (<http://www.ore.fr/>) (Braun et al., 2005). Our results  
79 show that the deep vadose zone plays a major role in buffering the groundwater response to  
80 the water percolation.

81

## 82 **Site description**

83

84 The study site is situated in South India (Figure 1), at 11° 44' N and 76° 27' E (Karnataka  
85 state, Chamrajnagar district).

86

### 87 *Figure 1: Location map of the experimental site*

88

89 It is located in the transition zone of a steep climatic and geomorphologic gradient at the edge  
90 of the rifted continental passive margin of the Karnataka Plateau, which was the focus of  
91 extensive geomorphologic studies (Gunnell and Bourgeon, 1997). This plateau, developed on  
92 the high-grade metamorphic silicate rocks of the West Dharwar craton (Moyen et al., 2001),  
93 is limited westward by the Western Ghâts, a first order mountain range. This mountain forms  
94 an orographic barrier, inducing an steep climatic gradient, with annual rainfall decreasing  
95 from west to east from about 6000 mm to 500 mm within a distance of about 80 km (Pascal,  
96 1982). These Ghâts are of critical ecological and economical importance and also an  
97 important source of all major South Indian rivers, flowing eastward towards the Gulf of  
98 Bengal. The climatic transition zone is mainly covered by dry deciduous forests, belonging to

99 the wildlife sanctuaries of Mudumalai, Waynad, Bandipur and Nagarahole (Prasad and  
100 Hedge, 1986). Such a tropical climosequence is comparable, although much steeper (Gunnell,  
101 2000), to the well documented monsoonal West African and the Northeast Brazilian  
102 climosequences (Gunnell, 1998).

103

104 The Mule Hole experimental watershed (4.1 km<sup>2</sup>) is located in the climatic semi-humid  
105 transition area and the mean annual rainfall (n = 25 years) is 1120 mm. The mean yearly  
106 temperature is 27 °C. On the basis of the aridity index defined as the ratio of mean annual  
107 precipitation to potential evapotranspiration, the climate regime can be classified as humid  
108 (UNESCO, 1979). Nevertheless, the climate is characterized by the occurrence of a marked  
109 dry season (around 5 months from December to April) and by recurrent droughts, depending  
110 on the monsoon rainfalls. The rainfall pattern is bimodal, as it is affected by both the South  
111 West Monsoon (June to September) and the North East Monsoon (October - December)  
112 (Gunnell and Bourgeon, 1997). Streams are ephemeral, and their flow duration ranges from a  
113 few hours to a few days after the storm events.

114

115 The watershed is mostly undulating with gentle slopes and the elevation of the watershed  
116 ranges from 820 to 910 m above sea level (Figure 1). The morphology of the watershed is  
117 convexo-concave highly incised by the temporary stream network. The lithology,  
118 representative of the West Dharwar craton (Naqvi and Rogers, 1987), is dominated by  
119 complexly folded, heterogeneous Precambrian peninsular gneiss intermingled with mafic and  
120 ultramafic rocks of the volcano-sedimentary Sargur series (Shadakshara Swamy et al., 1995).  
121 The Peninsular gneiss represents at least 85% of the watershed basement and the average  
122 strike value is N80°, with a dip angle ranging from 75° to the vertical (Descloitres et al.,  
123 2008). In such hard-rock context, the aquifer can generally be divided into two parts: one

124 upper part is the porous clayey to loamy regolith with an apparent density lower than the rock  
125 bulk density, the other is in the fractured-fissured protolith with an apparent density close to  
126 the bulk density of the rock and a network of fractures of a density decreasing with depth  
127 (Sekhar et al., 1994, Maréchal et al., 2004 ; Wyns et al., 2004 ; Dewandel et al., 2006). In the  
128 Mule Hole watershed, the average depth of the regolith is 17 m, as estimated through an  
129 extensive geophysical and geochemical survey (Braun et al., 2006 ; Braun et al., 2008). The  
130 distribution of the regolith depth (Figure 2) shows that the range of variation is 5 to 27 m. No  
131 correlation with the position on the hillslope was found. Average total porosity of the regolith  
132 is around 12%. Magnetic Resonance Sounding (MRS) performed on the watershed  
133 (Legchenko et al., 2006) showed that drainage porosity is around 1% in the regolith and  
134 below the detection level (<0.5%) in the fractured rock. Finally, timelapse geophysical  
135 measurements of both ERT and MRS conducted at the outlet of the watershed indicated a  
136 seasonal infiltration of water under the stream (Descloitres et al., 2008). A hydrological  
137 investigations allowed estimating the indirect recharge from the stream at around 30 mm.year<sup>-1</sup>  
138 at the watershed scale (Maréchal et al., 2009).

139

140 ***Figure 2 : distribution of regolith depth across the Mule Hole watershed (from a***  
141 ***geophysical and geochemical survey by Braun et al., 2008)***

142

143 The soil distribution in the watershed was determined by Barbiéro et al. (2007). The gneissic  
144 saprolite, cohesive to loose sandy, crops out both in the streambed and at the mid-slope in  
145 approximately 22% of the watershed area. The lower part of the slope and the flat valley  
146 bottoms (12% of the area) are covered by black soils (Vertisols and Vertic intergrades), which  
147 are 2 m deep on an average. Shallow red soils (Ferralsols and Chromic Luvisols), which are  
148 of 1 to 2 m deep, cover 66% of the entire watershed area. The watershed is covered by a dry

149 deciduous forest with different facies linked to the soil distribution (Barbiéro et al., 2007).  
150 Minimal human activity is present as it belongs to the Bandipur National Park, dedicated to  
151 wildlife and biodiversity preservation. The predominant tree component of the vegetation  
152 consists of *Anogeissus-Terminalia-Tectona* association (ATT facies) forming a relatively  
153 open canopy not exceeding 20 m (Prasad and Hedge, 1986 ; Pascal, 1986). Phenology is  
154 marked by a strong seasonality, with leaf senescence starting in December and leaf flushing  
155 occurring in early April, one or two month before the first significant monsoon rains. This  
156 surprising behaviour, leading to a deciduous period of only 2-3 months, much shorter than the  
157 dry season, is a general feature of the Asian forests (Singh and Kushawaha, 2005), and was  
158 quoted as the “paradox of Asian monsoon forest” by Elliot et al. (2006).

159

## 160 **Model description**

161

162 The model COMFORT (**CO**nceptual **M**odel for hydrological balance in **FOR**ested  
163 catchments) proposed in this article allows simulating the daily water budget of a forested  
164 watershed, through a simple and widely accepted conceptual description of the hydrological  
165 processes. It includes a lumped model for the soil moisture and the evapotranspiration in the  
166 forest (Granier et al., 1999), a surface runoff model based on the variable source area theory  
167 (Moore et al., 1983 ; Beven, 2001) and linear reservoirs for the recharge and groundwater  
168 discharge (Beven, 2001 ; Putty and Prasad, 2000). Its originality relies on the introduction of  
169 an additional water reservoir located in the weathered vadose zone (saprolite) below the soil,  
170 accessible to tree roots but not to understorey vegetation roots.

171

172 *Figure 3 : A schematic representation of the model COMFORT*

173

174 The model includes two modules, calibrated and run successively (Figure 3): the first one is a  
175 slightly modified and simplified version of the lumped water balance model presented by  
176 Granier et al (1999), which simulates the daily water balance for the forested soil and the  
177 surface runoff  $Q_s$ , while the second one simulates the flow of water through the deep vadose  
178 zone and the groundwater flow. Forcing variables are the daily rainfall (Rf), the Penman  
179 potential evapotranspiration (PET), and the forest leaf area index (LAI). The details of each of  
180 these modules is given below.

181

### 182 *Module 1: Soil moisture*

183

184 This module computes the daily variations in the soil moisture deficit (SMD, in mm) as:

185

$$186 \Delta SMD = E_{in} + T + E_u + PR + Q_s - Rf$$

187

188 and

189

$$190 0 < SMD < SMD_{max}$$

191

192 with  $E_{in}$  ( $\text{mm}\cdot\text{day}^{-1}$ ) being the evaporation of rainfall intercepted by the forest canopy,  $T$   
193 ( $\text{mm}\cdot\text{day}^{-1}$ ) the tree transpiration,  $E_u$  ( $\text{mm}\cdot\text{day}^{-1}$ ) the evapotranspiration of the understorey  
194 layer,  $PR$  ( $\text{mm}\cdot\text{day}^{-1}$ ) is the percolation below the soil layer, also called “potential recharge”  
195 by De Vries and Simmers (2002),  $Q_s$  ( $\text{mm}\cdot\text{day}^{-1}$ ) the surface runoff,  $Rf$  ( $\text{mm}\cdot\text{day}^{-1}$ ) the  
196 rainfall and  $SMD_{max}$  (mm) the maximum soil water deficit, equivalent to the soil water  
197 holding capacity.

198

199 The throughfall ( $R_f - E_{In}$ ) on the saturated area of the watershed (SA in %) reaches the stream  
200 as surface runoff ( $Q_s$  in  $\text{mm.day}^{-1}$ ) :

201

$$202 \quad Q_s = ( R_f - E_{In} ) \times SA / 100$$

203

204 Saturated area is usually computed as a function of water storage in the soil and the  
205 groundwater (see for example Putty and Prasad, 2000). In our context, groundwater level is  
206 far below the ground level, thus SA is modelled as an exponential function of the soil  
207 moisture deficit:

208

$$209 \quad SA = SA_{\max} \times \exp ( - a \times SMD )$$

210

211 with  $SA_{\max}$  the maximal extension of the saturated area (%), and  $a$  being the exponent  
212 constant. The proportion (%) of the soil surface covered by tree leaves ( $\varepsilon$ ) is calculated from  
213 the forest LAI with the Beer-Lambert function assuming a light coefficient of extinction of  
214 0.5 (Granier et al. 1999).

215

$$216 \quad \varepsilon = 1 - e^{-0,5 \times LAI}$$

217

218 The evaporation of rainfall intercepted by the forest canopy, or interception losses,  $E_{In}$   
219 ( $\text{mm.day}^{-1}$ ) is computed as:

220

$$221 \quad E_{In} = \text{minimum} ( \varepsilon \times R_f ; \varepsilon \times PET ; \varepsilon \times In )$$

222

223 with  $I_n$  (mm) the canopy storage capacity. This equation implies that canopy cannot store  
224 water for more than one day, and thus interception losses are nil during non rainy days. This  
225 simplification is justified by the fact that  $I_n$  is generally smaller than PET at a daily time step.

226

227 As proposed by Granier et al. (1999), to account for the fact that the rate of evaporation of  
228 intercepted water is approximately four time greater than transpiration rate (Rutter, 1967),  
229 PET is reduced by 20 % of the amount of intercepted water and the total actual  
230 evapotranspiration (AET) is limited to  $1.2 \times PET$ . The tree transpiration from the soil layer  
231 ( $T_s$  in  $\text{mm}\cdot\text{day}^{-1}$ ) is then calculated as:

232

$$233 \quad T_s = \text{minimum} (SMD_{\text{max}} - SMD ; (\epsilon \times PET) - (0,2 \times E_{In}) ; 1.2 \times PET - E_{In})$$

234

235 with  $SMD_{\text{max}}$  the maximum soil water deficit (mm), equivalent to the soil water holding  
236 capacity. In their model, Granier et al. (1999) propose that  $T/PET$  ratio decreases linearly  
237 when soil moisture reaches a critical level of 40% of the water holding capacity of the soil. In  
238 our model, for the sake of simplicity, transpiration is only limited by the amount of water  
239 present in the soil reservoir.

240

241 Evapotranspiration from understorey vegetation is calculated as:

242

$$243 \quad E_u = \text{minimum} (SMD_{\text{max}} - SMD - T_s ; (1-\epsilon) \times PET ; 1.2 \times PET - T_s - E_{In})$$

244

245 Actual evapotranspiration from the soil layer (AETs in  $\text{mm}\cdot\text{day}^{-1}$ ) is then:

246

$$247 \quad AET_s = E_{In} + T_s + E_u$$

248

249 Eventually, the water in excess in the soil reservoir (when  $SMD < 0$ ) percolates below the soil  
250 layer, as “potential recharge” ( $PR$  in  $mm \cdot day^{-1}$ ). This flow is an input to the weathered zone  
251 reservoir (module 2).

252

### 253 ***Module 2: Weathered zone and groundwater***

254

255 This module simulates the daily variations of the moisture deficit in the weathered zone  
256 ( $WZMD$  in  $mm$ ) as :

257

$$258 \Delta WZMD = T_{WZ} + R - PR$$

259

260 where  $T_{WZ}$  is the tree transpiration from the weathered zone below the soil ( $mm \cdot day^{-1}$ ),  $PR$  the  
261 potential recharge calculated in the module 1 ( $mm \cdot day^{-1}$ ) and  $R$  ( $mm \cdot day^{-1}$ ) the recharge. The  
262 potential evapotranspiration from the weathered zone ( $mm \cdot day^{-1}$ ) is the residual of the  
263 potential transpiration of trees minus the actual tree transpiration in the soil zone:

264

$$265 PET_{WZ} = \varepsilon \times PET - (0,2 \times E_{In}) - T_s$$

266

267 The actual transpiration from the weathered zone  $T_{WZ}$  ( $mm \cdot day^{-1}$ ) is then:

268

$$269 T_{WZ} = \text{minimum} (WZMD_{\max} - WZMD ; PET_{WZ})$$

270

271 with  $WZMD_{\max}$  ( $mm$ ) the maximum water deficit of the weathered zone.

272 Recharge ( $R_{WZ}$  in  $\text{mm}\cdot\text{day}^{-1}$ ) is the water in excess in the weathered zone (when  $WZMD < 0$ ).

273 To account for the observed smoothness of the recharge process,  $R_{WZ}$  is directed to a recharge

274 reservoir  $R$  (mm), and the effective recharge ( $R_{GW}$  in  $\text{mm}\cdot\text{day}^{-1}$ ) reaching the groundwater

275 reservoir (GW in mm) is calculated as :

276

$$277 \quad R_{GW} = \alpha_1 \times R$$

278

279 with  $\alpha_1$  ( $\text{day}^{-1}$ ) the recession coefficient of the recharge reservoir  $R$ .

280

281 Eventually, the daily variation of water content in the groundwater reservoir (GW in mm) is

282 calculated as:

283

$$284 \quad \Delta GW = R_{GW} - Q_{GW}$$

285

286 with the  $Q_{GW}$  the groundwater flow ( $\text{mm}\cdot\text{day}^{-1}$ ) calculated as :

287

$$288 \quad Q_{GW} = \alpha_2 \times GW$$

289

290 with  $\alpha_2$  ( $\text{day}^{-1}$ ) the recession coefficient of the groundwater reservoir  $GW$ . As the groundwater

291 level is always deeper than the stream bed at the outlet, this flow is considered as an

292 underflow.

293

294 The groundwater table level ( $L_{GW}$  in meters above sea level) is then calculated as:

295

$$296 \quad L_{GW} = L_0 + GW / (Sy \times 1000)$$

297

298 with  $L_0$  (masl) the altitude of the base of the aquifer and  $S_y$  its specific yield.

299

### 300 **Data acquisition and model calibration procedure**

301

302 The climatic data (daily rainfall and PET) necessary to run the model were available for the  
303 period 2003-2007 from the automatic weather station (CIMEL, type ENERCO 407 AVKP)  
304 installed at the Mulehole forest check post, which is 1.5 km West to the watershed outlet  
305 (Figure 1). Daily rainfall data were available at the same location from 1976 to 1995 from  
306 Indian Meteorological Department. Daily rainfall data were also available from the  
307 Ambalavayal weather station, located 20 km west of the study site, for the years 1979 to  
308 2004. As statistical analysis showed a strong correlation between the two stations, the seven  
309 missing years (1996-2002) in the Mule Hole were inferred from the Ambalavayal data.  
310 Granier et al. (1999) have shown that soil water content can be equally simulated in forest  
311 stands under different climates either with models based on Penmann potential  
312 evapotranspiration or with mechanistic approaches taking into account the canopy structure.  
313 Although many studies have shown that evapotranspiration is greater from forest than for the  
314 short size vegetation (Zhang et al., 2001) this difference is mainly attributed to better access  
315 to soil water at depth. Thus Penmann potential evapotranspiration was used as a forcing  
316 variable to the model.

317

318 As year to year variations in PET were little during the years 2003 to 2007, an average daily  
319 PET series was calculated and applied to the period 1976-2002. Using an average annual  
320 curve of PET does not affect much the rainfall-runoff models (Burnash, 1995 ; Oudin et al.,  
321 2005). The simulations were run on the reconstructed time series 1976-2007. Stream

322 discharge ( $Q_s$ ) is measured since August 2003 at a 6 minutes time step using a flume built at  
323 the outlet of the watershed. Due to technical problems, level recording was not available from  
324 15<sup>th</sup> April 2007 to 7<sup>th</sup> August 2007. A set of 13 observation wells were drilled in the area in  
325 2003 (P1-P6) and 2004 (P7-P13) (Figure 1). Most of these wells are dedicated to the  
326 monitoring of the effects of water seepage from the stream. Wells P2, P3, P5, P6, P9 and P10  
327 are not influenced by the indirect recharge from the stream (Maréchal et al., 2009), and can be  
328 used to assess the direct recharge. The water levels are monitored in all the wells either  
329 manually at a monthly time step or automatically at an hourly time-step. Due to technical  
330 problems (among which elephant attacks), P2 and P9 didn't give reliable records and were not  
331 included in the analysis. Additional data from an observation well (OW9) monitored by the  
332 Department of Mines and Geology (Karnataka State) since 1975, and located 20 km east of  
333 the watershed, which is close to the forest border, was used in the analysis.

334

335 As no measurement of forest leaf surface were carried out in the watershed, the evolution of  
336 LAI was hypothesised from qualitative observations from the site and references from  
337 literature concerning local tree phenology (Prasad and Hedge, 1986 ; Sundarapandian et al.,  
338 2005) and NDVI records for Indian forests (Prasad et al., 2005). Seasonality of leaf flushing  
339 and senescence is mostly driven by photoperiod, and therefore can be taken as a constant from  
340 one year to the other (Elliot et al., 2006 ; Singh and Kushwaha, 2005). The proposed LAI  
341 pattern is presented in the Figure 4a along with  $\epsilon$  variations. The comparison with the average  
342 monthly rainfall and PET over 32 years period (Figure 4b) shows that maximum PET is  
343 reached during the deciduous period and that on average, rainfall exceeds PET during five  
344 months.

345

346 *Figure 4: a) daily forest LAI and coefficient of extinction  $\varepsilon$ , b) average monthly rainfall*  
347 *(Rf) (1976-2007) and PET (2003-2007). Vertical bars indicate standard deviation of Rf.*

348

349 The two modules were run and calibrated successively, and the model performance was  
350 assessed using the Nash & Sutcliffe (1970) efficiency criterion. The module 1 is calibrated  
351 against the observed stream discharge values. This module has three forcing variables (Rf,  
352 PET and LAI) and four parameters ( $In$ ,  $a$ ,  $SA_{max}$  and  $SMD_{max}$ ). As the sensitivity analysis  
353 showed that the model was little sensitive to  $In$  value, it was set at 1 mm and calibration was  
354 performed on the three remaining parameters. The time series obtained for the potential  
355 evapotranspiration from the weathered zone ( $PET_{wz}$ ) and the potential recharge (PR) are then  
356 used as forcing variables for the module 2, which includes five parameters ( $WZMD_{max}$ ,  $\alpha_1$ ,  $\alpha_2$ ,  
357  $Sy$  and  $L_0$ ). The module 2 is calibrated for each piezometer against observed water table  
358 levels. To minimize equivalence possibilities, the following procedure was adopted: because  
359  $WZMD_{max}$  determines the date of initial water table rise, it is first adjusted by trial and error;  
360 then the four remaining parameters are automatically calibrated, with  $Sy$  values constrained  
361 smaller than 0.01, according to the conclusions of MRS survey (Legchenko et al., 2006). For  
362 each calibration, the solver was run with contrasting sets of initial parameter values, which  
363 later converged towards the same solution.

364

## 365 **Results**

366

367 *Figure 5: observed (black line) and simulated (grey line) daily surface runoff ( $Qs$  in*  
368  *$mm.day^{-1}$ ) at the Mule Hole watershed outlet for the 5 years of monitoring. Secondary axis*  
369 *is daily rainfall (Rf) in mm.*

370

371 The Figure 5 compares the observed and the simulated surface runoff ( $Q_s$ ) at the Mule Hole  
372 watershed outlet for the 5 years of monitoring. The Nash-Sutcliffe parameter calculated using  
373 the monthly values is 74. Despite this relatively low value, the model was able to reproduce  
374 the general trend of observed runoff, in particular the delay between the first monsoon rains  
375 and the first observed stream runoff. On the other hand, it was unable to reproduce the runoff  
376 observed after summer storm events in 2005, because they are due to Hortonian flow, a  
377 mechanism that was not accounted for in the model. However, this kind of event is of  
378 marginal importance in this pedoclimatic context. Considering that rainfall is measured in  
379 only one weather station located outside the watershed and the high spatial variability of  
380 rainfall, especially during strong individual storms, a perfect fit was not expected. In  
381 particular in 2005, two events, on 22<sup>nd</sup> of October and 4<sup>th</sup> of November, produced  $34 \text{ mm}\cdot\text{day}^{-1}$   
382  $^1$  and  $20 \text{ mm}\cdot\text{day}^{-1}$  of runoff for rains of  $52 \text{ mm}\cdot\text{day}^{-1}$  and  $28 \text{ mm}\cdot\text{day}^{-1}$  respectively. For these  
383 events, the actual rainfall in the watershed was probably much higher than the measured one.  
384 This is likely to have affected the assessment of water balance for the year 2005, as these two  
385 storms represent about one quarter of the total yearly runoff. However, this kind of event  
386 remains very rare: during the five monitoring years, only these two events produced more  
387 than 20mm of runoff, and only five other individual events produced more than 10 mm of  
388 runoff.

389

390 The calibrated parameter values are:  $a = 0.1$ ,  $SA_{\max} = 33.3\%$  and  $SMD_{\max} = 173 \text{ mm}$ . The  
391 value of maximal saturated area is probably overestimated, considering that the flat valley  
392 bottom overlaid by black soil occupies about 12% of the watershed area. The two exceptional  
393 storm events mentioned above played an important role in this overestimation. The calibrated  
394 value of  $SMD_{\max}$  is consistent with the soil moisture monitoring carried out in 2004 and 2005

395 in the site, showing a maximum variation of volumetric water content of 7% in red and black  
396 soils (Barbiéro et al., 2007) and an average 2 m depth (Braun et al., 2006).

397

398 ***Table 1 : Soil water balance (mm.year<sup>-1</sup>) for the monitored year and yearly average for the***  
399 ***monitored period and the whole 32 year simulated period. Signification of terms is in the***  
400 ***text. \*2003-2006 average***

401

402 Annual soil water balances as well as averages for the monitoring period and the 32 years  
403 simulation period are presented in the Table 1. Evapotranspiration is the most important sink  
404 for water, accounting for about 70% of rainfall. Interception is about 10% of rainfall, which is  
405 in the range of references values given in the literature for broad leaved forests (Ward and  
406 Robinson, 2000). Potential recharge is large (197 mm.year<sup>-1</sup> on the whole period), and  
407 displays an important year to year variability. It is larger than the estimate based on the  
408 regression equation proposed by Rangarajan and Athavale (2000) from tritium injection  
409 experiments in granitic areas in India, which gives a value of about 150 mm.year<sup>-1</sup> for the  
410 conditions of Mule Hole. This difference might be due to specificities of the study site, in  
411 particular the relatively low PET, mainly due to low temperatures linked with the altitude and  
412 to the forested environment which contributes to decrease soil compaction and increase  
413 infiltration potential (Bruijnzeel, 2004; Ilstedt et al., 2007). Results also show that the  
414 monitoring period is quite representative of the whole 32 years period with respect to the soil  
415 water balance.

416

417 ***Figure 6 : relative variation of water table level in hillslope piezometer, compared to***  
418 ***simulated potential recharge. Reference values for water table depth are 16.8 m, 27.8 m,***  
419 ***39.1 m and 37.4 m for P10, P3, P5 and P6 respectively.***

420

421 The Figure 6 compares the simulated daily potential recharge with observed relative  
422 variations in the water table level in hillslope piezometers. Although all piezometers showed a  
423 consistent global tendency to water level rise, they displayed significant contrasted behaviour.  
424 The relatively shallow piezometer (P10) responded each year to recharge, and the water level  
425 rise was almost simultaneous with the first occurrence of the potential recharge. Then the  
426 water level variation pattern was smooth, and the yearly maximum level was reached each  
427 year about two months after the end of the potential recharge period. For P3, the water table  
428 level did not increase in 2004, however showed a steep increase at the end of the 2005 rainy  
429 season, followed by a gentle continuous increase. In this well, ephemeral water table  
430 variations suggest the occurrence of some preferential flow (from August to October in 2006  
431 and 2007). Finally, the deep piezometers P5 and P6 displayed a declining tendency in 2004  
432 and 2005, a stabilisation or a very gentle rise in 2006, and a marked rise at the end of the rainy  
433 season 2007. These contrasted patterns of water table variation among the different hillslope  
434 piezometers suggest that they are linked with local processes and not by a regional aquifer  
435 dynamics.

436

437 ***Figure 7: Observed (dots) and simulated (lines) water level (in meter above sea level) in***  
438 ***piezometer P3, P5 and P10 for the monitoring period.***

439

440 ***Table 2 : Model parameters for the 3 simulated piezometers.***

441

442 Comparison of the observed and the simulated water level variations in piezometers for the  
443 monitoring period show a very good agreement (Figure 7), with Nash criteria values of 96.7,  
444 94.1 and 95.0 for P10, P3 and P5 respectively. Calibrated parameters (Table 2) are relatively

445 similar for the three piezometers. The most contrasted parameter is  $WZMD_{max}$ , the maximum  
446 water deficit of the weathered zone, because it accounts for the observed very long lag-time  
447 between water table rise observed in P10 in comparison with P3 (more than one year) and  
448 with P5 (more than 3 years). The calibrated value of the specific yield is consistent with the  
449 values obtained in similar fractured rock context in the region (Sekhar et al. 2004 ; Sekhar and  
450 Ruiz, 2006 ; Maréchal et al., 2006).

451

452 The most surprising result is the small value of the recession coefficient of the recharge  
453 reservoir ( $\alpha_1$ ). The recharge flow reaching the groundwater table is then very smooth, and it is  
454 mostly compensated by the groundwater discharge. The consequence is that the variations in  
455 the water content of the deep vadose zone (regolith and recharge reservoirs) are very large,  
456 with a maximum range of variation for the entire 32 year period of 650 mm, 745 mm and 851  
457 mm for P10, P3 and P5 respectively. Although very large, these variations are compatible  
458 with the material porosity, considering the depth of this vadose zone (from 15 m to 40 m).

459

460 ***Figure 8 : Simulated variations of water table level (in masl) in piezometer P3, P5 and P10***  
461 ***for the 32 year simulation period (lines). Dots represent observed values.***

462

463 ***Table 3: Watershed balance components (in  $mm \cdot year^{-1}$ ) for the piezometers P10, P3 and***  
464 ***P5, for the monitoring period and the 32 year simulation and average watershed balance***  
465 ***components calculated by weighted average (see text) .***

466

467 Average water balances components for each piezometer during the monitoring period and  
468 the 32 years simulation period are presented in the Table 3. Unlike the observations for the  
469 soil water balance, the monitored period appears dryer than the entire period. This is due to

470 the fact that the effects of the drought period from 2001 to 2003 persist longer at depth, which  
471 is apparent from the late rising of the deepest piezometers. The simulated long term variations  
472 of piezometers (Figure 8) reveals an alternance of wet and dry phases, of 12-15 years duration  
473 period. Maximum level in P5 is reached 2 to 3 years later than in P10. This simulated pattern  
474 was compared to the data recorded by the Department of Mines and Geology (Karnataka  
475 State) from 1974 to 2007 in a shallow observation well located outside the forest zone 20 km  
476 east of the study site. Although at the annual scale the observation well is much more reactive  
477 than P10, they display a very similar long-term trend. This observation suggests that the  
478 model was able to describe reasonably the global long-term behaviour of the groundwater.

479

480 ***Figure 9 : Simulated variations of water table level (in masl) in piezometer P10 (black line,***  
481 ***left Y-axis) and water level (depth to ground level in meters) recorded by Department of***  
482 ***Mines and Geology from 1974 to 2007 in a shallow observation well located outside the***  
483 ***forest zone 20 km east of the study site (grey line with dots, right Y-axis)***

484

485 Figure 10 illustrates the simulated variations of evaporation and transpiration during two  
486 years. It shows that transpiration by trees from the soil layer is the dominant flux during most  
487 of the year, especially during rainy season. Soil evapotranspiration by the understorey  
488 vegetation can be significant during dry season, depending on the occurrence of isolated rainy  
489 events. Transpiration of water from the deep weathered zone occurs mainly during dry  
490 season, and during dry periods on the course of the monsoon season. Because the model  
491 computes transpiration successively from soil and then from the weathered zone, the latter can  
492 occur only when soil water is completely depleted, leading to abrupt alternances between the  
493 two fluxes (figure 10c), which are probably much smoother in reality.

494

495 *Figure 10: Example of simulated daily evapotranspiration fluxes (in mm.day<sup>-1</sup>) compared*  
496 *to PET during two years a) variations of LAI b) Ein and Eu c) Ts and Twz (see text for*  
497 *signification of abbreviations)*

498

499 With an objective to obtain an assessment of the water balance at the watershed scale, we  
500 need to assess the representativity of the monitored piezometers with respect to the entire  
501 area. The parameter WZMD<sub>max</sub>, which is driving the most important part of the observed  
502 piezometer variability, is probably linked with the regolith depth in the vicinity of the  
503 piezometer. P10 is located in an area where the regolith depth is around 8m, P3 around 15 m  
504 and P6 more than 20m. A resistivity logging performed on P5 suggested a regolith depth of  
505 22m (Braun et al., 2008). As a first approach, we can consider that P10, P3 and P5 are  
506 representative of area with regolith depth of 0-12m, 12-18m and more than 18m respectively.  
507 According to the regolith depth distribution in the watershed (Figure 2), the proportion is  
508 30%, 27% and 43% for P10, P3 and P5 respectively. With this hypothesis, the watershed  
509 balance (Table 3) appears roughly equilibrated during the 32 years simulation period, while  
510 the water gain was 125 mm.year<sup>-1</sup> during the monitoring period. The average water uptake by  
511 trees from the deep weathered zone is 104 mm, and average groundwater underflow is 78  
512 mm.year<sup>-1</sup>. Groundwater recharge is equivalent to underflow on the long term. This value is  
513 close to the recharge that was assessed in this area with Chloride mass balance method (45  
514 mm.year<sup>-1</sup>, Maréchal et al., 2009).

515

## 516 **Discussion**

517

518 The 5 years monitoring allowed us to give a tentative assessment of the water balance of a  
519 small experimental watershed using a simple conceptual lumped model. However, the

520 exercise has proven to be difficult, due to the climatic context and the presence of forest. The  
521 plausibility of the model results and the future work needed to validate them are discussed in  
522 this section.

523

524 One uncertainty is linked to the assessment of evapotranspiration in forest stands. This issue  
525 continues to generate a great deal of controversy in the literature (Andreassian, 2004 ;  
526 Bruijnzeel, 2004 ; Robinson et al., 2003). The difficulty is also greater for regions with the  
527 index of dryness (PET/Rf) close to 1.0 (Zhang et al., 2004), which is the case in our study  
528 site. However, despite its limitations, the Penman-Montieth PET approach has proven its  
529 ability to simulate soil water moisture in a broad range of climatic conditions and tree species  
530 (Granier et al., 1999). The average total evapotranspiration found in our long term simulations  
531 (around 900 mm.year<sup>-1</sup>, out of which about 100 mm are linked to extra transpiration by deep  
532 tree roots, see Table 3) is in very good agreement with the worldwide evapotranspiration  
533 curve proposed for forests and grasslands by Zhang et al. (2001). In our climatic context,  
534 water percolation towards the deep vadose zone is mainly concentrated during short rainy  
535 periods of the monsoon season, usually few days to two weeks, followed by drier periods. In  
536 this configuration, soil water budget is less sensitive to evapotranspiration assessment.  
537 However, direct measurements of forest evapotranspiration would allow a better calibration of  
538 the model.

539

540 According to our model, the spatial variability of the water reservoir located at depth in the  
541 weathered zone and accessible to deep roots of trees is a key parameter for water budgeting in  
542 semi-arid forested watersheds. Our calibration gave values ranging from 50 to 470 mm (Table  
543 2). Few studies have been dedicated to measure the hydraulic properties of weathered granitic  
544 rocks (Jones and Graham, 1993; Katsura et al., 2006). They suggest that weathered rocks have

545 the capacity to hold appreciable amount of water that is available to plants (Jones and  
546 Graham, 1993 ; Williamson et al., 2004). The fact that tree roots are able to uptake water at  
547 considerable depth, especially in water limited ecosystems is widely accepted (Nepstad et al.,  
548 1994 ; Canadell et al., 1996 ; Collins and Bras, 2007). Importance of water storage in deep  
549 weathered rock in forested ecosystems has recently gained recognition, and large scale  
550 surveys to quantify deep water reservoirs have been attempted, for example in Cambodia  
551 (Ohnuki et al., 2008), leading to estimates as high as 1350 mm. The average total porosity of  
552 the saprolite in the Mule Hole watershed was estimated at 12% from geophysical and  
553 geochemical studies (Braun et al., 2008). Even assuming that the proportion of the porosity  
554 available to plants is only 5%, considering a 16 m deep saprolite would lead to an average  
555 water storage capacity of 800 mm, which is compatible with our findings. Considerable  
556 spatial variability of water stress and tree mortality during drought period is commonly  
557 reported in dry deciduous forests (Nath et al., 2006). A survey dedicated to check whether  
558 part of this variability can be explained by the regolith depth would constitute a validation of  
559 our hypothesis.

560

561 The most surprising consequence of the model calibration is the great importance of the  
562 recharge reservoir, and its low recession coefficient. In temperate regions, recharge process is  
563 usually considered to be very quick, and in most models water percolated below the soil zone  
564 is immediately transferred to the groundwater. This is acceptable because groundwater table is  
565 generally shallow, and the regolith matric porosity is filled every year by recharge. However,  
566 the fact that matric water can drain for a long time is well documented (Healy and Cook,  
567 2002). In a chalk aquifer, Price et al. (2000) demonstrated that the delay between recharge  
568 period and the smooth water table rise can be explained by matric water storage in the vadose  
569 zone, which is slowly released to groundwater during dry periods. By monitoring water

570 content variations in a 21m deep sandstone vadose zone, Rimón et al. (2007) found a  
571 variation of 660 mm of water content during a rainy season, and a slow decrease in water  
572 content during the dry season. In a hydrogeologic survey in Australia, in a granitic  
573 environment, Ghauri (2004) observes a long delay between rainfall and groundwater  
574 response, attributed to matrix storage in the deep vadose zone. If this hypothesis is confirmed,  
575 it could be of considerable importance for water resource evaluation in hard rock aquifers,  
576 because in most cases recharge is assessed through water table level methods (Healy and  
577 Cook, 2002). Monitoring of water content variations in the deep vadose zone of our  
578 experimental watershed would allow validating this hypothesis.

579

580 The modelled watershed balance leads to an average water flow of about  $180 \text{ mm}\cdot\text{year}^{-1}$ , out  
581 of which 80 mm is groundwater underflow. This underflow might reach the streams of higher  
582 order rivers, like Nugu Hole or Kabini (Figure 1). Indeed, it is very small compared to the  
583 estimates of the flows produced in the humid zone of the climatic gradient that range from  
584  $900$  to  $4700 \text{ mm}\cdot\text{year}^{-1}$  (Putty and Prasad, 2000). However, these high flows are produced  
585 during the rainy season, and during the dry season rivers virtually dry up (Putty and Prasad,  
586 2000). Because groundwater underflow from transition area produces a fairly constant load,  
587 it might be of significant importance in sustaining the baseflow in large rivers during the dry  
588 season. This will be assessed through a regional modelling in a future work.

589

## 590 **Conclusions**

591

592 This study is based on a five years monitoring of an experimental forested watershed in the  
593 South India, and using a conceptual model of the water balance over a 32 years period  
594 allowed us to draw the following conclusions :

595 i) In tropical forest ecosystems, deciduous trees can uptake a significant amount of water from  
596 the deep regolith. This mechanism is particularly important at the end of the dry summer  
597 period, because the leaf flushing can precede monsoon rains by several weeks. More  
598 investigations are needed to check if variability in regolith depth can be linked to the  
599 variability of tree mortality during dry periods in monsoon season.

600 ii) This water uptake, combined with the spatial variability of regolith depth, can account for  
601 the variable lag time between drainage events and groundwater rise observed for the different  
602 piezometers.

603 iii) Water table response to the recharge is buffered due to the long vertical travel time  
604 through the deep vadose zone, which constitutes a major water reservoir. The five years  
605 monitoring period reveals that the watershed water balance is not equilibrated, mainly due to  
606 large variations in water content in the vadose zone. This observation is of great importance  
607 for water resource assessment, as water level fluctuation method is often used to estimate  
608 yearly groundwater recharge, especially in India (G.E.C., 1997). Our results show that this  
609 method can lead to an underestimation of recharge when vadose zone is large.

610

611 This study stresses the importance of long term observatories for the understanding of the  
612 hydrological processes in tropical forested ecosystems.

613

#### 614 **Acknowledgements**

615 The Mule Hole basin is part of the ORE-BVET project (Observatoire de Recherche en  
616 Environnement – Bassin Versant Expérimentaux Tropicaux, [www.orebvet.fr](http://www.orebvet.fr)). Apart from the  
617 specific support from the French Institute of Research for Development (IRD), the Embassy  
618 of France in India and the Indian Institute of Science, our project benefited of funding from  
619 IRD and INSU/CNRS (Institut National des Sciences de l'Univers / Centre National de la

620 Recherche Scientifique) through the French programmes ECCO-PNRH (Ecosphère  
621 Continentale: Processus et Modélisation – Programme National Recherche Hydrologique),  
622 EC2CO (Ecosphère Continentale et Côtière) and ACI-Eau. It is also funded by the Indo-  
623 French programme IFCPAR (Indo-French Center for the Promotion of Advanced Research  
624 W-3000). The multidisciplinary research carried on the Mule Hole watershed began in 2002  
625 under the control of the IFCWS (Indo-French Cell for Water Sciences), joint laboratory  
626 IISc/IRD. We thank the Department of Mines and Geology of Karnataka for providing data  
627 and the Karnataka Forest Department and the staff of the Bandipur National Park for all the  
628 facilities and support they provided.

629

630 **References**

631

632 Andréassian, V., 2004 Water and forests: from historical controversy to scientific debate.

633 Journal of Hydrology 291, 1-27.

634 Anuraga, T.S., Ruiz, L., Mohan Kumar, M.S., Sekhar, M. and Leijnse, T.A., 2006 Estimating

635 groundwater recharge using land use and soil data: a case study in South India.

636 Agricultural Water Management 84 (1-2) 65-76.

637 Barbiéro, L., Parate, H. R., Descloitres, M., Bost, A., Furian, S., Mohan Kumar, M.S., Kumar,

638 C., and Braun, J. J., 2007. Using a structural approach to identify relationships between soil

639 and erosion in a semi-humid forested area, south india. Catena 70(3), 313–329.

640 Beven, K.J., 2001. Rainfall-runoff modelling: the primer. Wiley, Chichester, 360p

641 Braun J.J., Ruiz L., Riotte J., Mohan Kumar M.S., Murari V., Sekhar M., Barbiéro L.,

642 Descloitres M., Bost A., Dupré B., Lagane C., 2005. Chemical and physical weathering in

643 the Kabini River Basin, South India. Geochimica Cosmochimica Acta 69 (10), A691-A691

644 Braun, J.J., Descloitres, M., Riotte, J., Barbiéro, L., Fleury, S., Boeglin, J.L., Ruiz, L., Muddu,

645 S., Mohan Kumar, M.S., Kumar, M.C., and Dupré, B., 2006. Regolith thickness inferred

646 from geophysical and geochemical studies in a tropical watershed developed on gneissic

647 basement: Moole Hole, Western Ghâts (South India). Geochimica et Cosmochimica Acta

648 70 (18), A65-A65

649 Braun, J.J., Descloitres, M., Riotte, J., Fleury, S., Barbiéro, L., Boeglin, J.L., Violette, A.,

650 Lacarce, E., Ruiz, L., Sekhar, M., Mohan Kumar, M.S., Subramanian, S. and Dupré, B.,

651 2008 Regolith mass balance inferred from combined mineralogical, geochemical and

652 geophysical studies: Mule Hole gneissic watershed, South India. Geochimica and

653 Cosmochimica Acta, <http://dx.doi.org/10.1016/j.gca.2008.11.013>

654 Bruijnzeel, L.A., 2004 Hydrological functions of tropical forests: not seeing the soil for the  
655 trees? *Agriculture, Ecosystems & Environment*, 104(1), 185-228.

656 Burnash, R.J.C., 1995. In: V.P. Singh, Editor, *The NWS river forecast system—catchment*  
657 *modeling*, Computer Models of Watershed Hydrology, Water Resources Publications,  
658 Highlands ranch, Co. 311–366.

659 Canadell, J., Jackson, R.B., Ehleringer, J.R., Mooney, H.A., Sala, O.E., Schulze, E.-D., 1996.  
660 Maximum rooting depth of vegetation types at the global scale. *Oecologia* 108, 583–595

661 Collins, D. B. G. and Bras, R. L., 2007. Plant rooting strategies in water-limited ecosystems.  
662 *Water Resources Research* 43, W06407

663 Descloitres, M., Ruiz, L., Sekhar, M., Legchenko, A., Braun, J.-J., Mohan Kumar, M. S., and  
664 Subramanian, S., 2008. Characterization of seasonal local recharge using electrical  
665 resistivity tomography and magnetic resonance sounding. *Hydrological Processes* 22(3),  
666 384-394.

667 De Vries, J.J., and Simmers, I., 2002. Groundwater recharge: an overview of processes and  
668 challenges. *Hydrogeology Journal* 10, 8–15.

669 Dewandel, B., Lachassagne, P., Wyns, R., Maréchal, J.C., Krishnamurthy, N.S., 2006. A  
670 generalized 3-D geological and hydrogeological conceptual model of granite aquifers  
671 controlled by single or multiphase weathering. *Journal of Hydrology* 330 (1-2): 260-284,  
672 doi:10.1016/j.jhydrol.2006.03.026.

673 Elliot, S., Baker, P.J. and Borchert, R., 2006. Leaf flushing during the dry season : the  
674 paradox of Asian monsoon forests. *Global ecology and biogeography* 15(3), 248-257.

675 G.E.C., 1997 *Groundwater Resource Estimation Methodology*. Report of the Groundwater  
676 Resource Estimation Committee, Ministry of Water Resources, Government of India, New  
677 Delhi, India, 100 pp

678 Ghauri, S. 2004 Groundwater trends in the Central Agricultural Region. Resource  
679 Management Technical Report 269. Department of Agriculture, Western Australia. 66p.

680 Granier, A., Bréda, N., Biron, P. and Vilette, S., 1999. A lumped water balance model to  
681 evaluate duration and intensity of drought constraints in forest stands. Ecological  
682 Modelling 116, 269-283.

683 Gunnell, Y. and Bourgeon, G., 1997. Soils and climatic geomorphology on the Karnataka  
684 plateau, peninsular India. CATENA 29, 239-262.

685 Gunnell, Y., 1998. Passive margin uplifts and their influence on climatic change and  
686 weathering patterns of tropical shield regions. Global and Planetary Change 18(1-2), 47-  
687 57.

688 Gunnell, Y., 2000. The characterization of steady state in Earth surface systems: findings  
689 from the gradient modelling of an Indian climosequence. Geomorphology 35, 11-20.

690 Healy, R.W. and Cook, P.G., 2002. Using groundwater levels to estimate recharge.  
691 Hydrogeology Journal 10(1) 91-109.

692 Ilstedt, U., Malmer, A., Verbeeten, E., Murdiyarso, D., 2007. The effect of afforestation on  
693 water infiltration in the tropics: a systematic review and meta-analysis. Forest Ecology and  
694 Management 251 (1–2), 45–51.

695 Jones, D.P. and Graham, R.C., 1993. Water-holding characteristics of weathered granitic rock  
696 in chaparral and forest ecosystems. Soil Science Society of America Journal 57, 256-261.

697 Katsura, S., Kosugi, K., Yamamoto, N. and Mizuyama, T., 2006. Saturated and unsaturated  
698 hydraulic conductivities and water retention characteristics of weathered granitic bedrock.  
699 Vadose Zone Journal 5(1), 35-47.

700 Legchenko, A., Descloitres, M., Bost, A., Ruiz, L., Reddy, M., Girard, J. P., Sekhar, M.,  
701 Mohan Kumar, M. S., and Braun, J.-J., 2006. Resolution of MRS applied to the  
702 characterization of hard-rock aquifers. Ground Water 44, 547-554.

703 Maréchal, J. C., Dewandel, B. and Subrahmanyam, K., 2004. Use of hydraulic tests at  
704 different scales to characterize fracture network properties in the weathered-fractured layer  
705 of a hard rock aquifer. *Water Resources Research* 40, W11508.

706 Maréchal, J.C., Dewandel, B., Ahmed, S., Galeazzi, L., and Zaidi, F.K., 2006. Combined  
707 estimation of specific yield and natural recharge in a semi-arid groundwater basin with  
708 irrigated agriculture. *Journal of Hydrology* 329(1-2), 281-293.

709 Maréchal, J.C., Varma, M.R.R., Riotte, J., Vouillamoz, J.M., Mohan Kumar, M.S., Ruiz, L.,  
710 Sekhar, M., Braun, J.J., 2009 Indirect and direct recharges in a tropical forested watershed:  
711 Mule Hole, India. *Journal of Hydrology*, 364 (3-4), 272-284.

712 Moore, I.D., Coltharp, G.B. and Sloan, P.G., 1983. Predicting runoff from small Appalachian  
713 watersheds. *Transactions of the Kentucky Academy of Sciences (USA)*, 44(3/4), 135-145

714 Moyen, J.F., Martin, H. and Jayananda, M., 2001. Multi-element geochemical modeling of  
715 crust-mantle interactions during late-Archean crustal growth: the Closepet Granite (South  
716 India). *Precambrian Research* 112 (1-2), 87-105.

717 Naqvi, S. M. and Rogers, J. W., 1987. *Precambrian geology of India*. Clarendon Press,  
718 Oxford University Press, New york.

719 Nash, J. E. and Sutcliffe, J. V., 1970. River flow forecasting through conceptual models. Part  
720 I. A discussion of principles. *Journal of Hydrology* 10 (3) 282–290.

721 Nath, C.D., Dattaraja, H.S., Suresh, H.S., Joshi, N.V. and Sukumar, R., 2006. Patterns of tree  
722 growth in relation to environmental variability in the tropical dry deciduous forest at  
723 Mudumalai, southern India. *Journal of Biosciences* 31, 651–669.

724 Nepstad, D.C., Carvalho, C.R., Davidson, E.A., Jipp, P., Lefebvre, P., Negreiros, G.H.d., da  
725 Silva, E.D., Stone, T.A., Trumbore, S. and Vieira, S., 1994. The role of deep roots in the  
726 hydrological and carbon cycles of Amazonian forests and pastures. *Nature* 372, 666–669.

727 Ohnuki, Y., Kimhean, C., Shinomiya, Y. and Toriyama, J., 2008. Distribution and  
728 characteristics of soil thickness and effects upon water storage in forested areas of  
729 Cambodia. *Hydrological Processes* 22, 1272-1280.

730 Oudin, L., Michel, C., and Anctil, F., 2005. Which potential evapotranspiration input for a  
731 lumped rainfall-runoff model? Part 1-Can rainfall-runoff models effectively handle  
732 detailed potential evapotranspiration inputs? *Journal of Hydrology* 303, 275–289.

733 Pascal, J.P., 1982. Forest map of South India, 1/250 000 scale, sheet Mercara–Mysore.  
734 Travaux Section Scientifique et Technique Institut Français de Pondichéry, hors série, vol.  
735 18a.

736 Pascal, J.P., 1986. Explanatory booklet on the forest map of South India. Travaux Section  
737 Scientifique et Technique Institut Français de Pondichéry, Hors Serie, vol. 18.

738 Prasad, V.K., Anuradha, E., Badinath, K.V.S., 2005. Climatic controls of vegetation vigor in  
739 four contrasting forest types of India-evaluating from National Oceanic and Atmospheric  
740 Administration's Advanced Very High Resolution Radiometer datasets (1990–2000).  
741 *International Journal of Biometeorology* 50, 6–16.

742 Prasad, S.N. and Hedge, M., 1986. Phenology and seasonality in the tropical deciduous forest  
743 of Bandipur, South India. *Proceedings of the Indian Academy of Sciences (Plant Sci.)*  
744 96(2), 121-133.

745 Price, M., Low, R. G., and McCann, C., 2000. Mechanisms of water storage and flow in the  
746 unsaturated zone of the Chalk aquifer. *Journal of Hydrology* 233(1-4), 54-71.

747 Putty, M.R.Y. and Prasad, R., 2000. Understanding runoff processes using a watershed model  
748 - a case study in the Western Ghats in South India. *Journal of Hydrology* 228, 215-227.

749 Rangarajan, R., and Athavale R.N., 2000. Annual replenishable ground water potential of  
750 India - an estimate based on injected tritium studies. *Journal of Hydrology*, 234(1-2), 38-  
751 53.

752 Rimon, Y., Dahan, O., Nativ, R. and Geyer S., 2007. Water percolation through the deep  
753 vadose zone and groundwater recharge: Preliminary results based on a new vadose zone  
754 monitoring system. *Water Resources Research* 43, W05402.

755 Robinson, M., Cognard-Plancq, A. -L., Cosandey, C., David, J., Durand, P., Fuhrer, H. -W.,  
756 Hall, R., Hendriques, M. O., Marc, V., McCarthy, R., McDonnell, M., Martin, C., Nisbet,  
757 T., O'Dea, P., Rodgers, M. and Zollner, A., 2003. Studies of the impact of forests on peak  
758 flows and baseflows: a European perspective. *Forest Ecology and Management* 186(1-3),  
759 85-97.

760 Rutter, A.J., 1967. An analysis of evaporation from a stand of Scots pine. In: Sopper, W.E.,  
761 Lull, H.W. (Eds.), *Forest Hydrology*. Pergamon Press, Oxford.

762 Scanlon, B.R., Healy, R.W. and Cook, P.G., 2002 Choosing appropriate techniques for  
763 quantifying groundwater recharge. *Hydrogeology Journal* 10(1) 18-39.

764 Scanlon, B.R., Keese, KE., Flint, AL., Flint, L E., Gaye, CB., Edmunds, W. M, and Simmers,  
765 I., 2006. Global synthesis of groundwater recharge in semiarid and arid regions.  
766 *Hydrological Processes* 20(15), 3335-3370.

767 Sekhar, M. and Ruiz, L., 2006. Regional Groundwater Modeling: A Case study of Gundal  
768 sub-basin, Karnataka, India. In Krishnaswamy, J., Lele, S. and Jayakumar, R. (Eds.)  
769 *Hydrology and Watershed Services in the Western Ghats of India: Effects of land use and*  
770 *land cover change*. Tata-McGraw-Hill, New Delhi, India. 81-103.

771 Sekhar, M., Rasmi, S.N., Sivapullaia, P.V. and Ruiz, L., 2004. Groundwater flow modeling of  
772 Gundal sub-basin in Kabini river basin, India. *Asian Journal of Water Environmental*  
773 *Pollution* 1 (1-2), 65-77.

774 Sekhar, M., Mohan Kumar, M.S. and Sridharan, K., 1994. Parameter estimation in an  
775 anisotropic leaky aquifer system. *Journal of Hydrology* 163, 373-391.

776 Shadakshara Swamy, N., Jayananda, M., and Janardhan, A. S., 1995. Geochemistry of  
777 Gundlupet gneisses, Southern Karnataka: a 2.5 Ga old reworked sialic crust. In: Yoshida,  
778 M., Santosh, M., and Rao, A. T. Eds.), India as a fragment of East Gondwana. Gondwana  
779 Research Group.

780 Singh, K.P. and Kushwaha, C.P., 2005. Emerging paradigms of tree phenology in dry tropics.  
781 Current Science 89(6) 964-975.

782 Sundarapandian, S.M., Chandrasekaran, S. and Swamy, P.S., 2005. Phenological behaviour of  
783 selected tree species in tropical forest at Kodayar in te Western Ghats, Tamil Nadu, India.  
784 Current Science 88(5) 805-810.

785 UNESCO, 1979. Map of the world distribution of arid regions, 54 pp, UNESCO, Paris.

786 Wagener, T., Wheeler H.S. and Gupta, H.V., 2004. Rainfall-runoff Modelling in Gauged and  
787 Ungauged Catchments. Imperial College Press, London, 300p

788 Ward, R.C. and Robinson, M., 2000. Principles of hydrology. McGraw-Hill, London (4<sup>th</sup>  
789 edition), 450p.

790 Williamson, T.N., Newman, B.D., Graham, R.C. and Shouse, P.J., 2004. Regolith water in  
791 zero-order chaparral and perennial grass watersheds four decades after vegetation  
792 conversion. Vadose Zone Journal 3(3),1007-1016.

793 Wyns, R., Baltassat, J.M., Lachassagne, P., Legchenko, A., Vairon, J. and Mathieu, F., 2004.  
794 Application of proton magnetic resonance soundings to groundwater reserve mapping in  
795 weathered basement rocks (Brittany, France). Bulletin de la Société Géologique de France  
796 175(1), 21-34.

797 Zhang, L., Dawes, W. R., and Walker, G. R., 2001. Response of mean annual  
798 evapotranspiration to vegetation changes at catchment scale. Water Resources Research  
799 37(3), 701–708.

800 Zhang, L., Hickel, K., Dawes, W. R., Chiew, F. H. S., Western, A. W. and Briggs, P. R.,  
801 2004. A rational function approach for estimating mean annual evapotranspiration. *Water*  
802 *Resources Research* 40, W02502, doi:10.1029/2003WR002710.

803 List of Figures:

804

805 Figure 1: Location map of the experimental site

806

807 Figure 2 : distribution of regolith depth across the Mule Hole watershed (from a geophysical  
808 and geochemical survey by Braun et al., 2008)

809

810 Figure 3 : A schematic representation of the model COMFORT

811

812 Figure 4: a) daily forest LAI and coefficient of extinction  $\epsilon$ , b) average monthly rainfall (Rf)  
813 (1976-2007) and PET (2003-2007). Vertical bars indicate standard deviation of Rf.

814

815 Figure 5: observed (black line) and simulated (grey line) daily surface runoff ( $Q_s$  in  $\text{mm}\cdot\text{day}^{-1}$ )  
816 <sup>1</sup>) at the Mule Hole watershed outlet for the 5 years of monitoring. Secondary axis is daily  
817 rainfall (Rf) in mm.

818

819 Figure 6 : relative variation of water table level in hillslope piezometer, compared to  
820 simulated potential recharge. Reference values for water table depth are 16.8 m, 27.8 m, 39.1  
821 m and 37.4 m for P10, P3, P5 and P6 respectively.

822

823 Figure 7: observed (dots) and simulated (lines) water level (in meter above sea level) in  
824 piezometer P3, P5 and P10 for the monitoring period.

825

826 Figure 8 : simulated variations of water table level (in masl) in piezometer P3, P5 and P10 for  
827 the 32 year simulation period (lines). Dots represent observed values.

828

829 Figure 9 : simulated variations of water table level (in masl) in piezometer P10 (black line,  
830 left Y-axis) and water level (depth to ground level in meters))recorded by Central  
831 Groundwater Board from 1974 to 2007 in a shallow observation well located in an  
832 agricultural zone 20 km east of the study site (grey line with dots, right Y-axis)

833

834 Figure 10: example of simulated daily evapotranspiration fluxes (in  $\text{mm}\cdot\text{day}^{-1}$ ) compared to  
835 PET during two years a) variations of LAI ; b)  $E_{in}$  and  $E_u$  ; c)  $T_s$  and  $T_{wz}$  (see text for  
836 signification of abbreviations)

837

838 List of tables :

839

840 Table 1 : Soil water balance ( $\text{mm}\cdot\text{year}^{-1}$ ) for the monitored year and yearly average for the  
841 monitored period and the whole 32 year simulated period. Signification of terms is in the text.

842 \*2003-2006 average

843

844 Table 2 : model parameters for the 3 simulated piezometers.

845

846 Table 3: watershed balance components (in  $\text{mm}\cdot\text{year}^{-1}$ ) for the piezometers P10, P3 and P5,  
847 for the monitoring period and the 32 year simulation and average watershed balance  
848 components calculated by weighted average (see text).

849

Figure 1  
[Click here to download high resolution image](#)

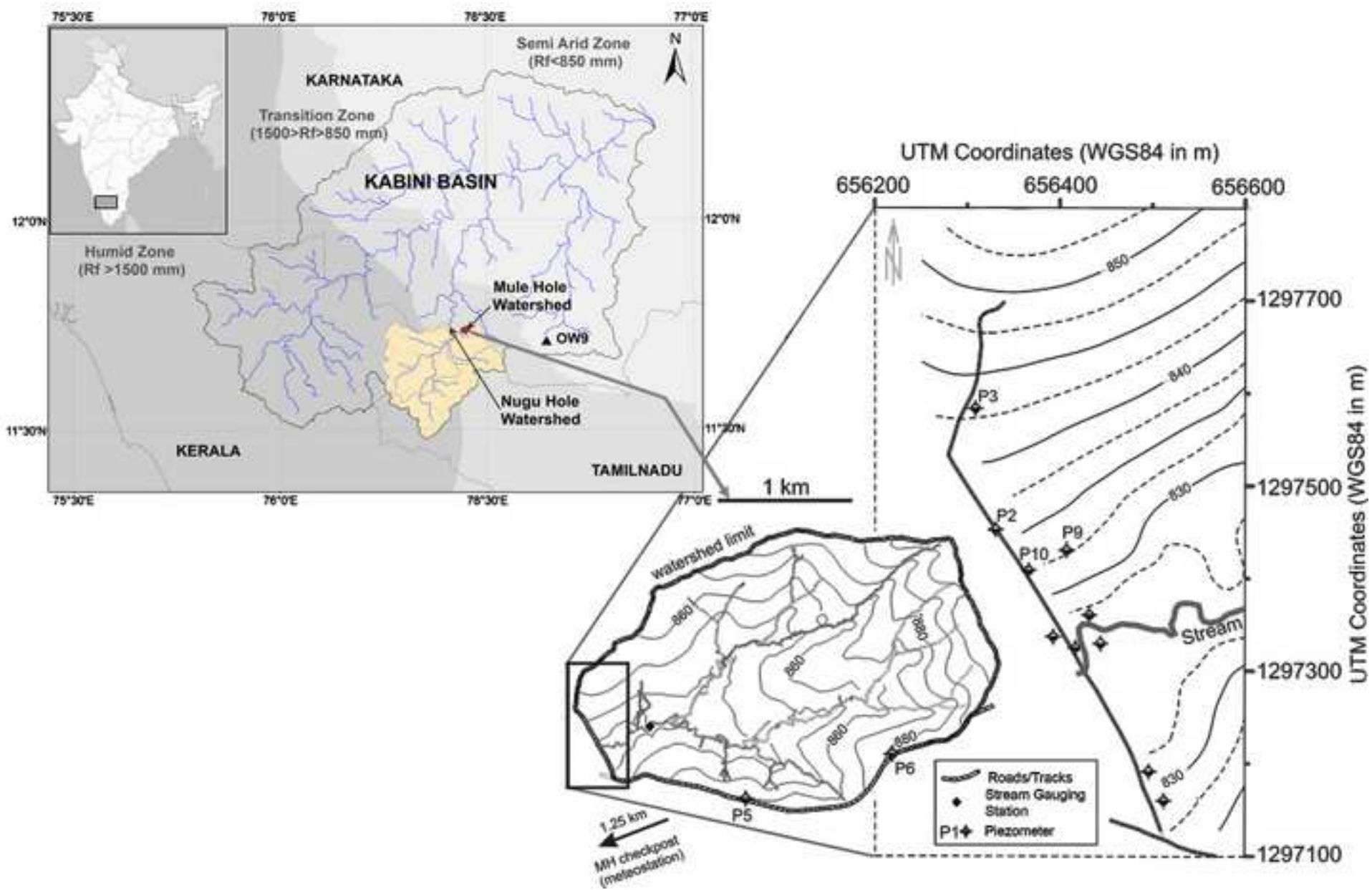


Figure 2  
[Click here to download high resolution image](#)

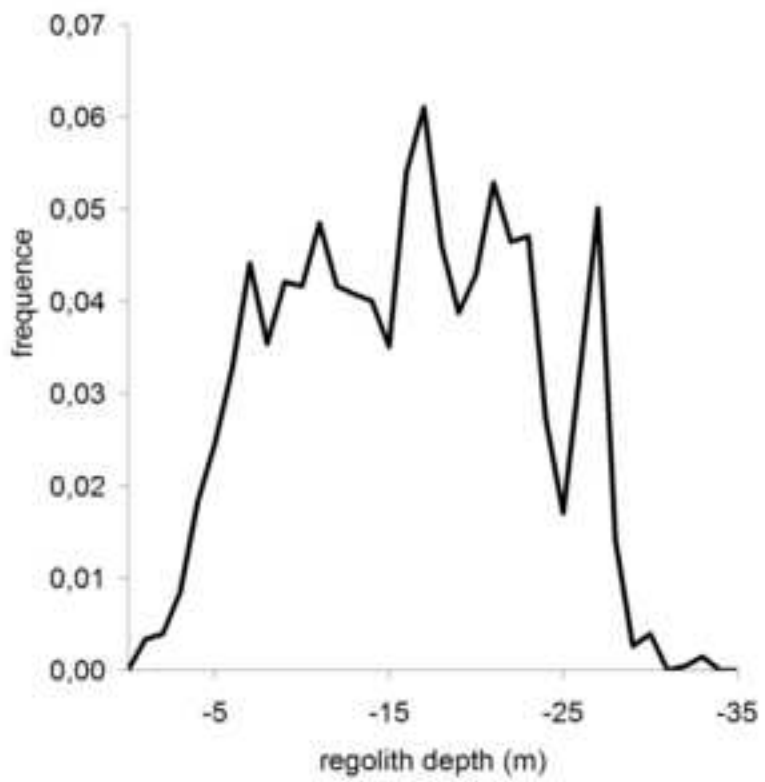


Figure 3

[Click here to download high resolution image](#)

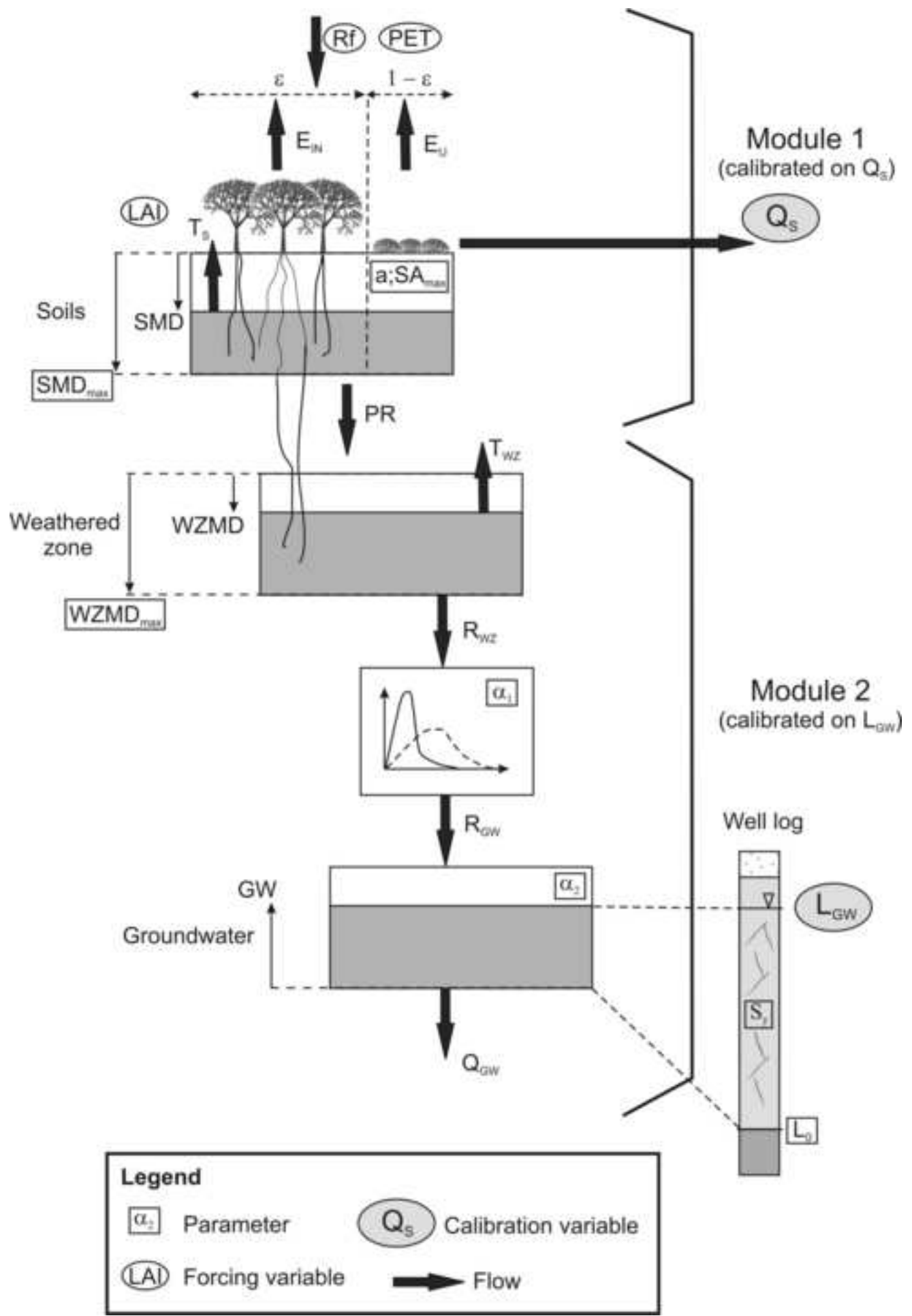


Figure 4

[Click here to download high resolution image](#)

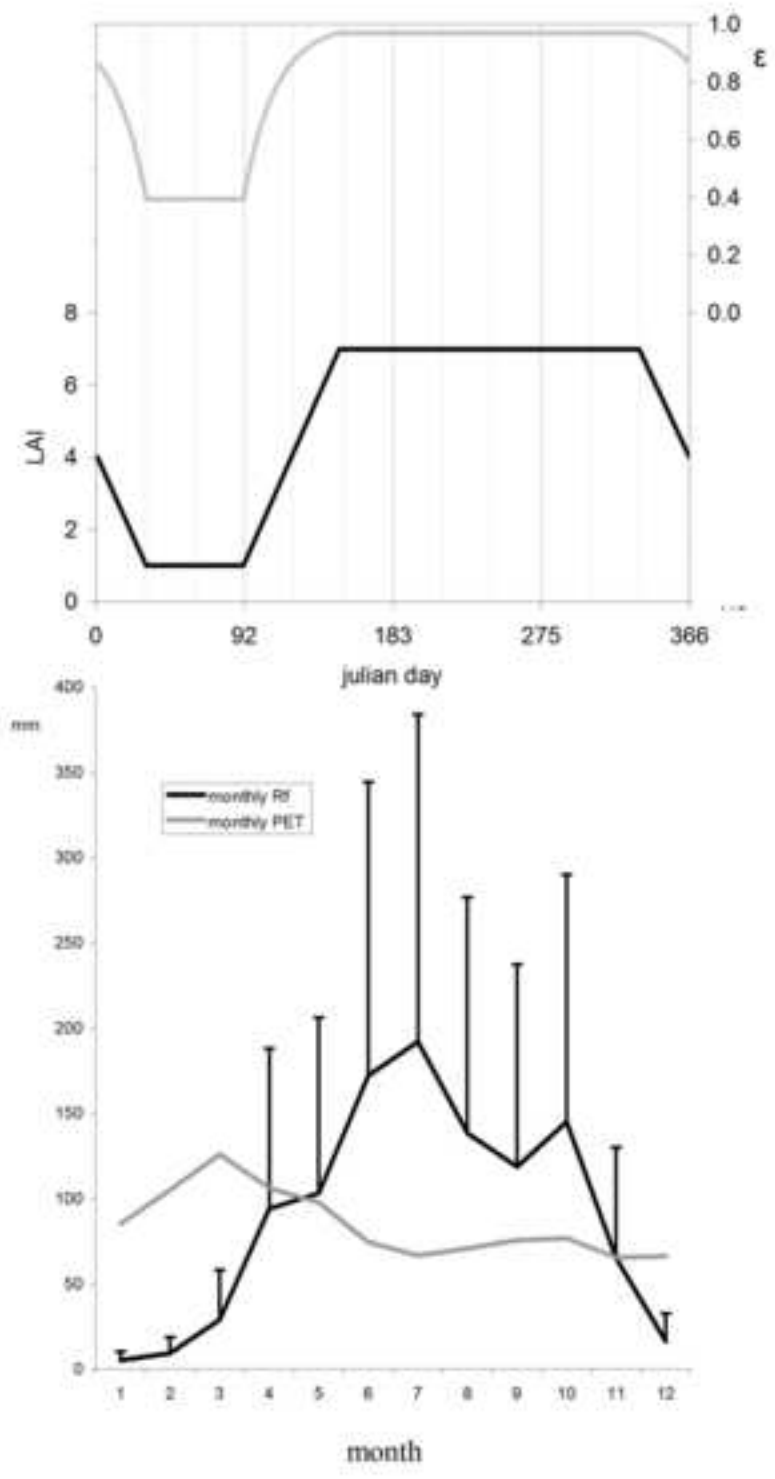


Figure 5  
[Click here to download high resolution image](#)

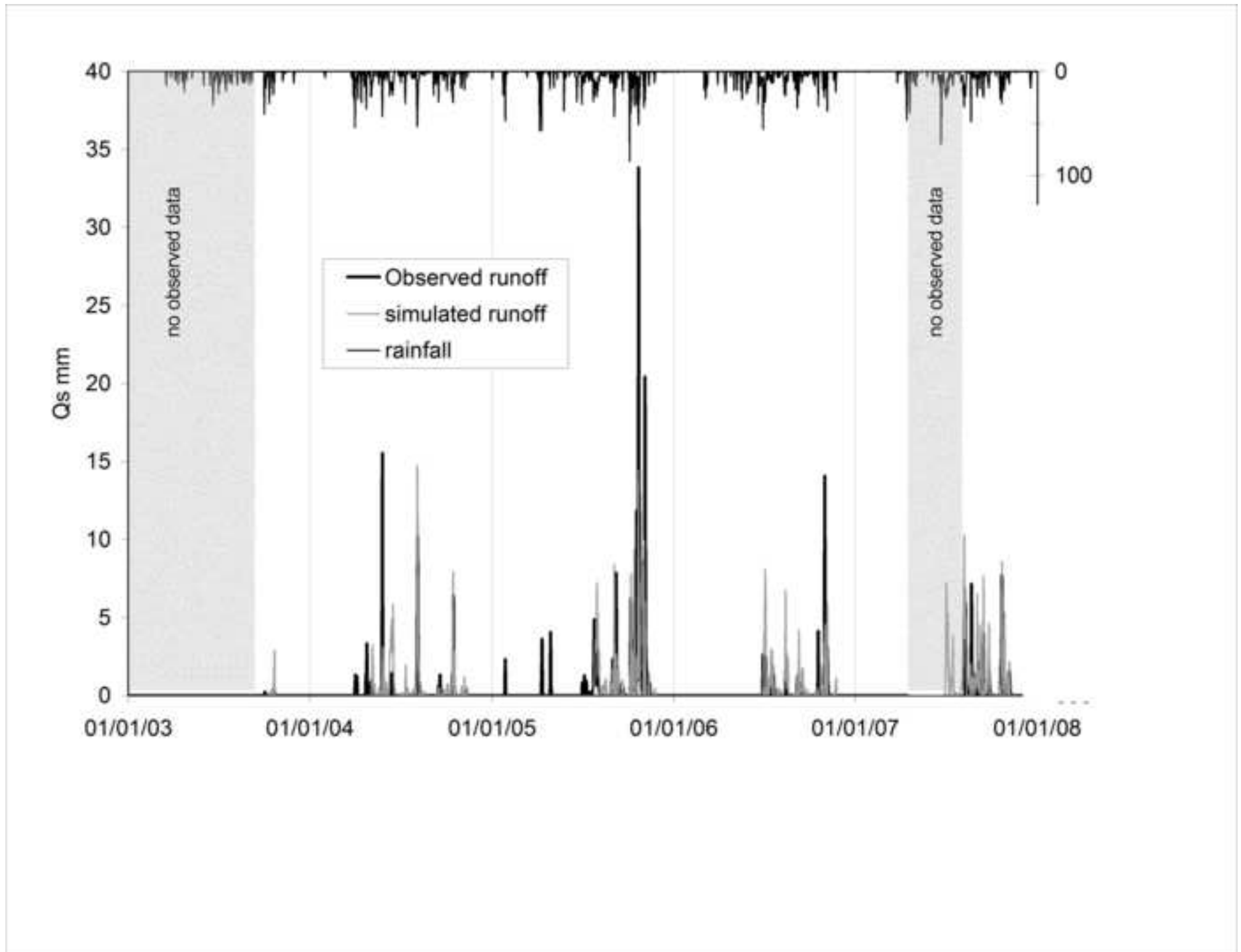


Figure 6  
[Click here to download high resolution image](#)

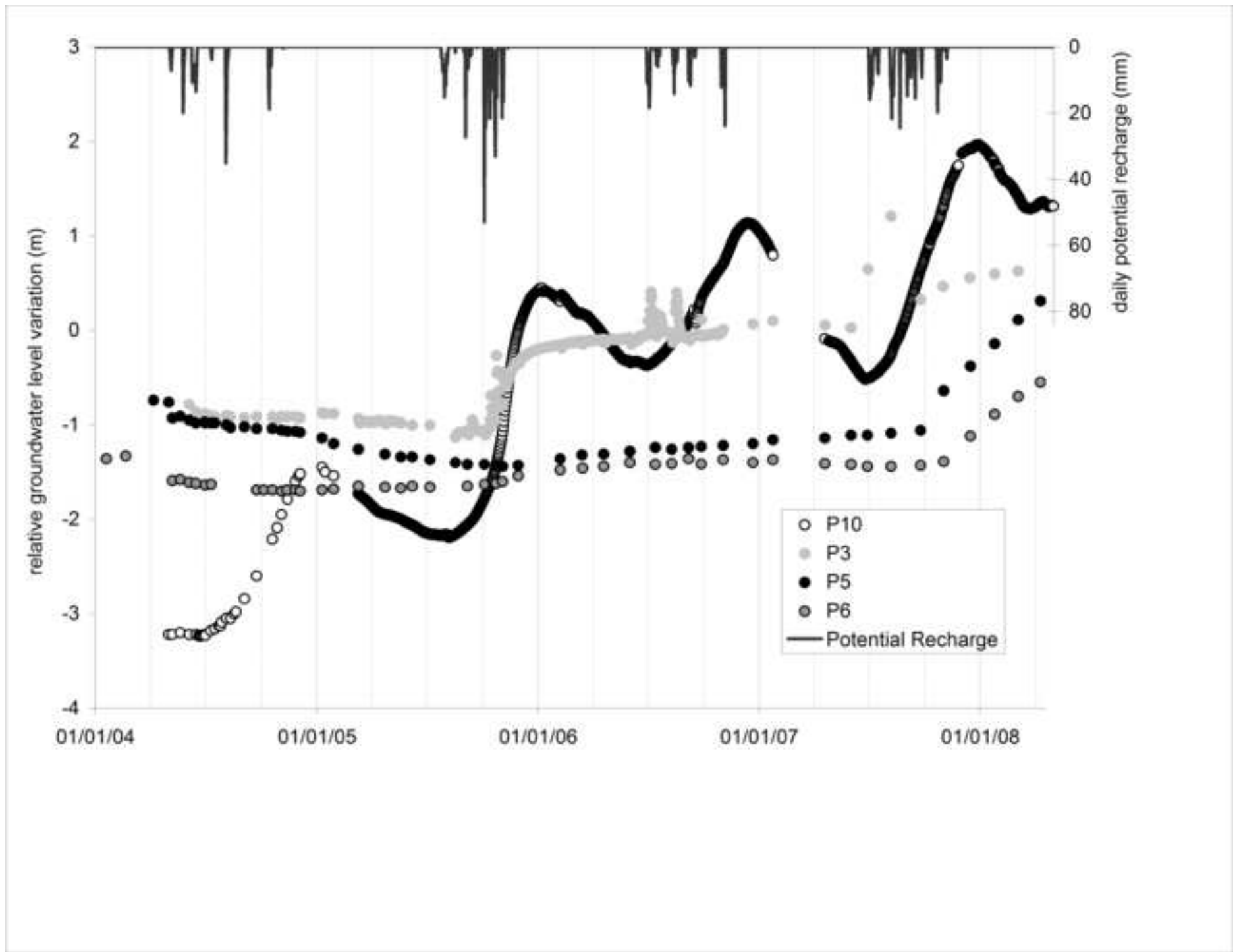


Figure 7  
[Click here to download high resolution image](#)

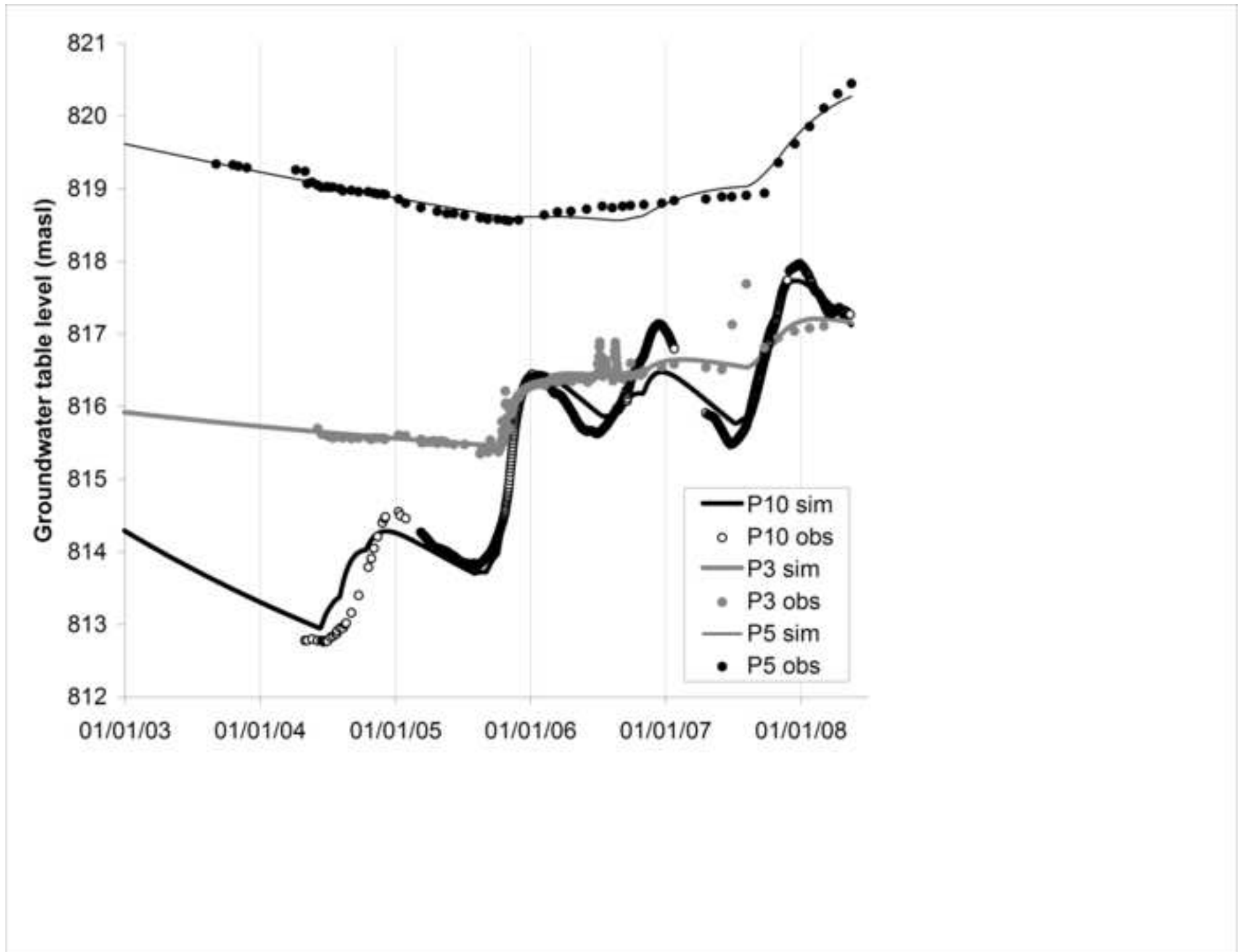


Figure 8  
[Click here to download high resolution image](#)

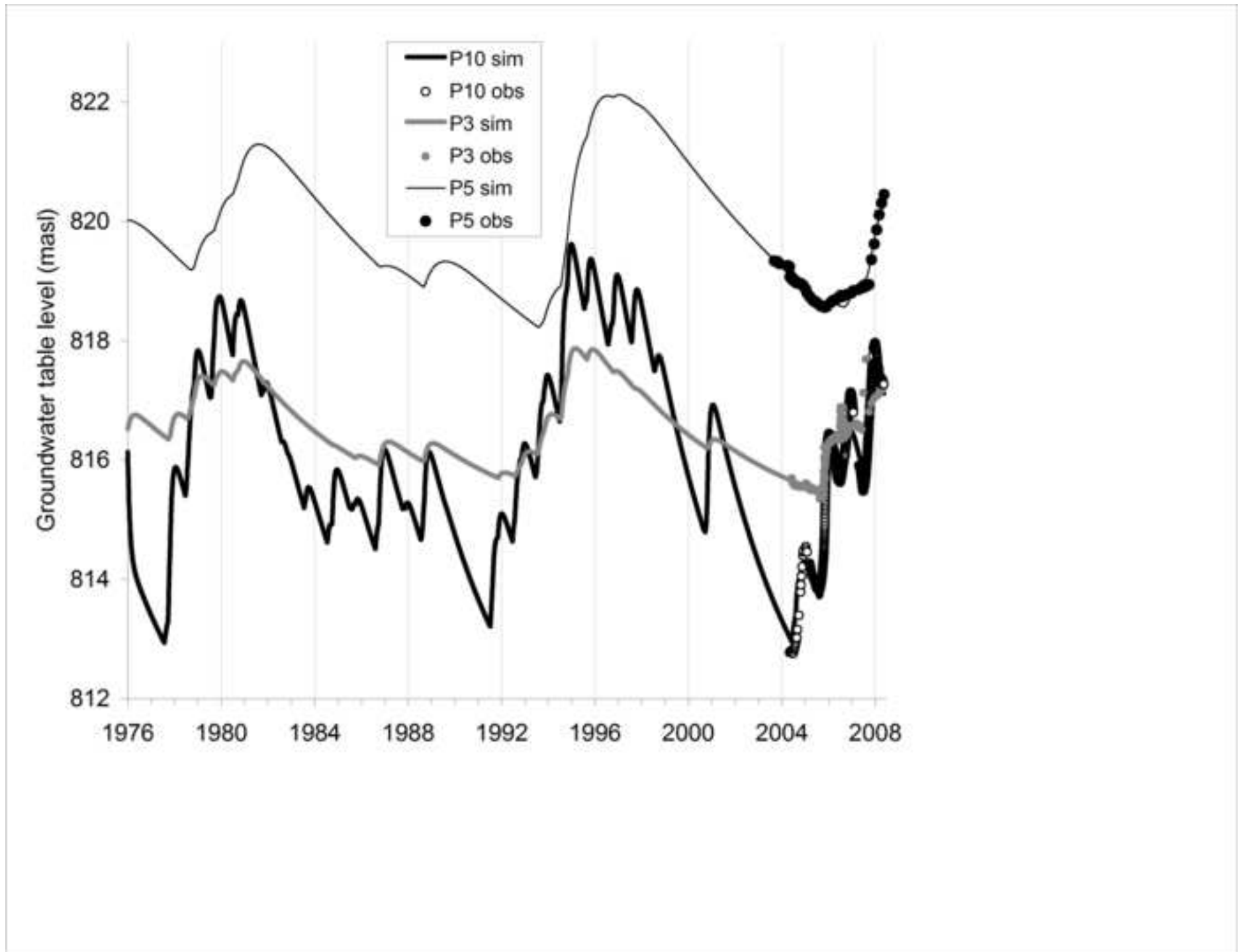


Figure 9  
[Click here to download high resolution image](#)

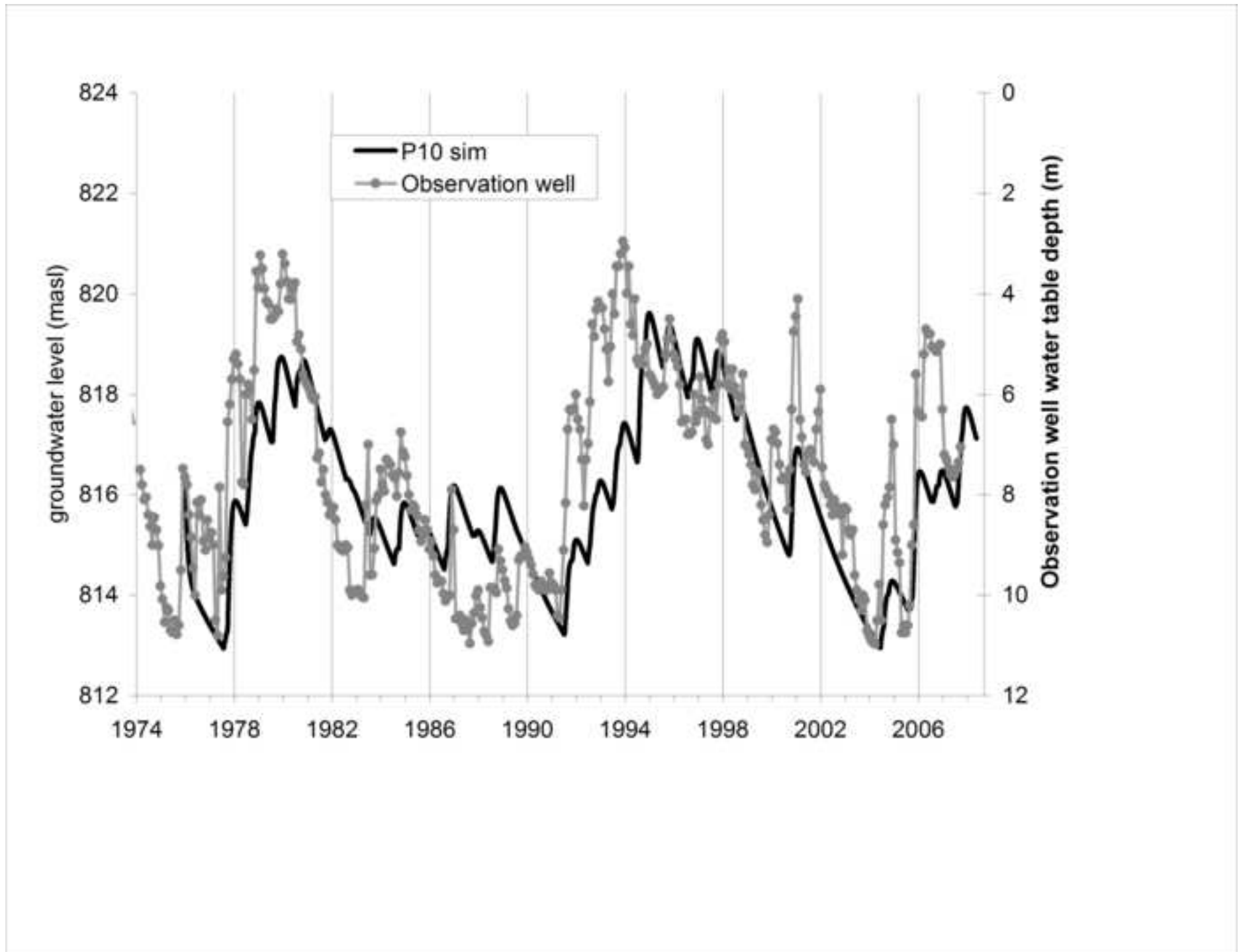
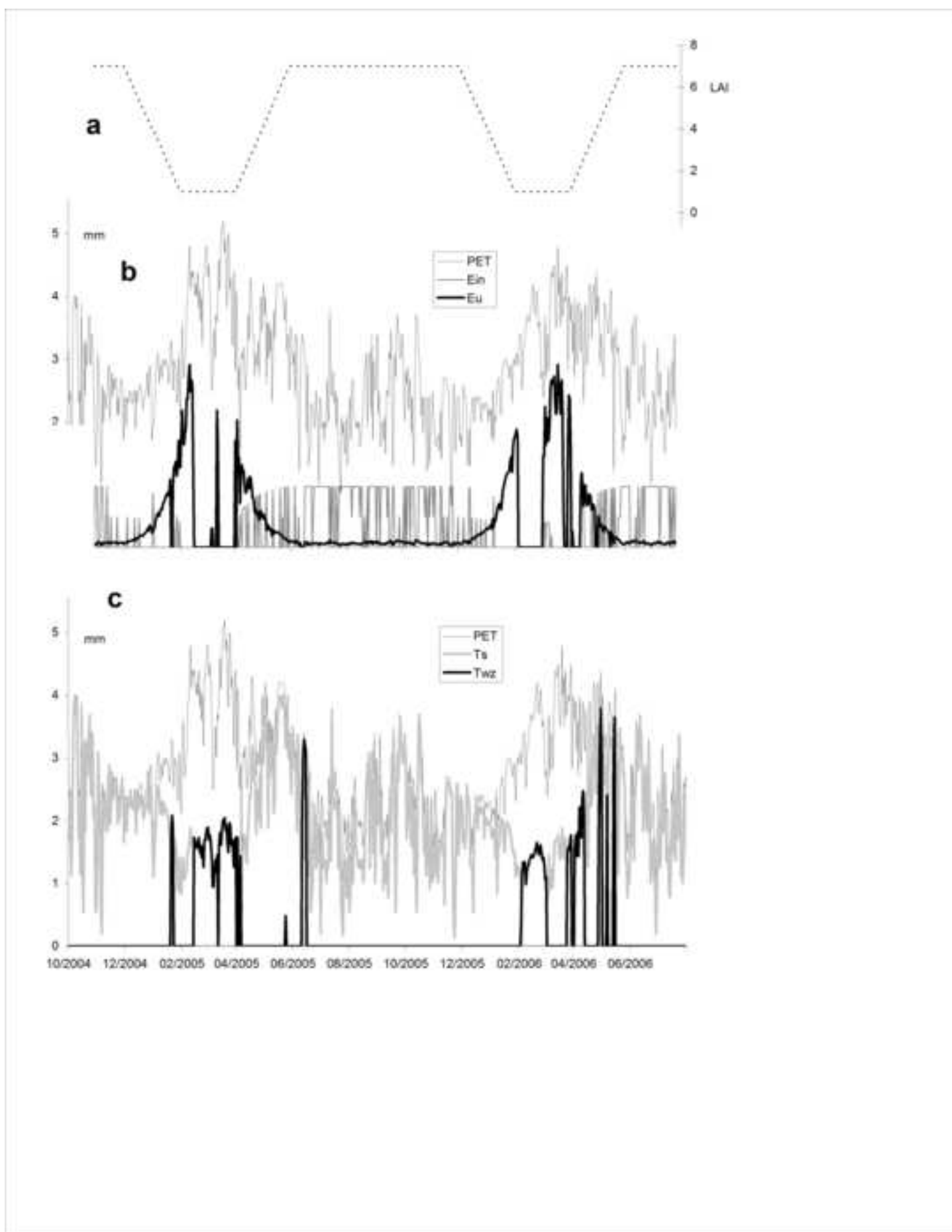


Figure 10

[Click here to download high resolution image](#)



	2003	2004	2005	2006	2007	2003-2007	cv %	1976-2007	cv %
<b>Rf</b>	706	1216	1434	1170	1252	1155	(23)	1091	(32)
<b>PET</b>	1101	1074	1017	1012	963	1034	(5)	1067	-
<b>E<sub>in</sub></b>	78	130	133	123	136	120	(20)	98	(23)
<b>E<sub>u</sub></b>	53	79	111	127	72	89	(34)	82	(33)
<b>T<sub>s</sub></b>	555	627	624	649	546	600	(8)	624	(11)
<b>AET<sub>s</sub></b>	686	837	868	900	754	809	(11)	803	(14)
<b>PR</b>	6	225	372	183	318	221	(64)	197	(87)
<b>PET<sub>wz</sub></b>	268	144	97	87	118	143	(51)	158	(58)
<b>Obs Qs</b>	1	66	196	52	-	79 *	(105)	-	-
<b>sim Qs</b>	5	117	154	92	162	93 *	(68)	94	(79)

Table 1 : Soil water balance (mm/year) for the monitored year and yearly average for the monitored period and the whole 32 year simulated period. Signification of terms is in the text.  
 \*2003-2006 average

	P10	P3	P5
Ground level (masl)	832.82	844.24	859.14
initial watertable depth (m)	16.82	27.75	39.14
<i>parameters:</i>			
L <sub>0</sub>	809.93	814.73	814.85
WZMD <sub>max</sub>	50	250	470
α <sub>1</sub>	6.96 10 <sup>-4</sup>	4.89 10 <sup>-4</sup>	2.32 10 <sup>-4</sup>
Sy	2.10 10 <sup>-3</sup>	6 10 <sup>-3</sup>	5.11 10 <sup>-3</sup>
α <sub>2</sub>	3.03 10 <sup>-2</sup>	1.71 10 <sup>-2</sup>	4.39 10 <sup>-3</sup>

Table 2 : model parameters for the 3 simulated piezometers.

	<b>2003-2007</b>	<b>cv %</b>	<b>1976-2007</b>	<b>cv %</b>
<b>Rf</b>	<b>1155</b>	<b>(23)</b>	<b>1091</b>	<b>(32)</b>
<b>AET<sub>s</sub></b>	<b>809</b>	<b>(11)</b>	<b>803</b>	<b>(14)</b>
<b>sim Q<sub>s</sub></b>	<b>107</b>	<b>(59)</b>	<b>94</b>	<b>(79)</b>
<i>Local balance</i>				
P10 T <sub>WZ</sub>	31	(83)	43	(52)
P10 Q <sub>GW</sub>	115	(28)	141	(26)
P3 T <sub>WZ</sub>	62	(89)	114	(53)
P3 Q <sub>GW</sub>	49	(38)	68	(35)
P5 T <sub>WZ</sub>	62	(89)	141	(47)
P5 Q <sub>GW</sub>	34	(8)	42	(22)
<i>Watershed balance</i>				
<b>T<sub>WZ</sub></b>	<b>53</b>	<b>(88)</b>	<b>104</b>	<b>(43)</b>
<b>Q<sub>GW</sub></b>	<b>62</b>	<b>(23)</b>	<b>78</b>	<b>(26)</b>
<i>water balance</i>	<b>125</b>	<b>(103)</b>	<b>12</b>	<b>(1346)</b>

Table 3: watershed balance components (in mm/year) for the piezometers P10, P3 and P5, for the monitoring period and the 31 year simulation and average watershed balance components.